



Monitoring and classification of karst rocky desertification with Landsat 8 OLI images using spectral indices, multi-endmember spectral mixture analysis and support vector machine

Çağan Alevkayalı ¹, Onur Yayla ², Yıldırım Atayeter ¹

¹Süleyman Demirel University, Geography Department, Türkiye

²Mehmet Akif Ersoy University, Department of Turkish and Social Sciences Education, Türkiye

Keywords

Remote sensing
Karst Rocky Desertification
Spectral Indices
Spectral Mixture Analysis
Machine Learning

Research Article

DOI: 10.26833/ijeg.1149738

Received:27.07.2022

Revised: 14.02.2023

Accepted: 16.03.2023

Published:08.05.2023



Abstract

Karst Rocky Desertification (KRD) is the reduction of vegetative productivity of this land with the release of bedrock as a result of the full or partial transportation of the fertile soil through natural processes and human activities in karst landscapes. The purpose of this study is to reveal the effectiveness of Remote Sensing methods in monitoring, mapping and evaluating KRD. Landsat 8 OLI images were used to carry out these procedures. In monitoring this process, Karst Bare Rock Index (KBRI), Normalized Difference Rock Index (NDRI), Carbonate Rock Index 2 (CRI2), Normalized Difference Build-Up Index (NDBI), Normalized Difference Vegetation Index (NDVI), Dimidiate Pixel Model (DPM), Multi Endmember Spectral Mixture Analysis (MESMA) and Support Vector Machine (SVM) were used from the spectral indices. In order to determine KRD with spectral indexes, a strong linear relationship was tested between some indices such as DPM ($R^2=0,79$), KBRI ($R^2=0,66$), and NDBI ($R^2=0,64$) and field measurements. In order to evaluate the results obtained, KRD was divided into 4 basic classes such as none, mild, moderate, and severe. According to these classification levels, it was determined that the SVM method had the highest accuracy ($Kappa=0.88$). According to the classification results, which have the highest accuracy in the study area, the rate of areas undergoing severe karst desertification is 40%, moderate desertification process is 17%, mild desertification is 14% and non-desertification is 29%. In the study, it was concluded that the KRD strengthens as one goes from south to north and from west to east in the research area. This study points out KRD is one of the effective ecosystem problems in the Mediterranean region, Türkiye.

1. Introduction

The concept of karst is defined as the process of dissolution and deposition realized on carbonates, evaporates and halite with water [1]. This term essentially explains the shapes that are created by the melting of soluble rocks and passing underground through surface streams [2]. The term karst has been associated with the world of science with the German pronunciation of the name of a region between Italy and Slovenia, which is called Carso in Italian and Kras in Slovenian [1]. Karst landscapes are characterized by landforms such as dolines, caves, collapsed sinkholes and carbonate deposits that develop on carbonate rocks (limestone, dolomite, marble) or evaporites (gypsum, anhydrite, rock salt) [2,3].

The total area of karst landscapes around the world is approximately 22 million km² which accounts for approximately 12% of the lithosphere [4,5]. Karst landscapes with heterogeneous and complex land cover, are among the different types of surfaces that make up the lithosphere, are widespread in Türkiye as well as in several parts of the world. Considering the spread of karst landscapes in Türkiye, it is known that these areas correspond to approximately one third of the total area of the country [6].

Karst regions have sensitive ecological characteristics due to geological structures [7]. In karst landscapes, fragmented plant communities that develop on discontinuous soil cover are generally encountered [8]. For this reason, when damage to the soil and vegetation in Karst regions cannot be tolerated in the

* Corresponding Author

(caganalevkayali@sdu.edu.tr) ORCID ID 0000-0001-7044-8183
(oyayla@mehmetakif.edu.tr) ORCID ID 0000-0002-8710-3701
(yatayeter@sdu.edu.tr) ORCID ID 0000-0002-7570-2993

Cite this article

Alevkayalı, Ç., Yayla, O., & Atayeter, Y. (2023). Monitoring and classification of karst rocky desertification with Landsat 8 OLI images using spectral indices, multi-endmember spectral mixture analysis and support vector machine. International Journal of Engineering and Geosciences, 8(3), 277-289

short term, the ecosystem in these regions suffers [9]. One of the most important problems that arise in the ecosystem in karst landscapes is the exposure of the bedrock after the soil cover has been removed due to the destruction of vegetation as a result of natural processes or human effects [10]. This process, which is defined as Karst Rocky Desertification (KRD) in the literature, actually refers to land degradation in karst landscapes in its simplest terms [4,10]. KRD, which means the reduction of soil cover due to deforestation and erosion in karst lands, is a term used to express a land degradation process [11]. According to the explanations in the literature, the erosion of the soil due to human activities such as crop production, animal grazing, extreme climatic events, and changes in land functions are the leading causes that accelerate KRD [12, 13, 7]. The negative effects caused by KRD are both environmental and economic problems such as landslides, floods and erosion [14]. The rapid development of many environmental problems in areas where KRD is effective is important in terms of identifying regions where this process has developed and controlling it by monitoring.

Vegetation cover, exposed bedrock and soil depth are used in expressing or classifying the degree of degradation of the land during the KRD process [11]. However, there is no standard approach to the classification of surfaces on which this problem is effective as regards monitoring, mapping or evaluation of KRD (Table 1). For example, in the study conducted by Yang et al. [13], the regions where the open rock surface is more than 70% in terms of KRD classification were stated as very severe desertification areas. On the other hand, the same surfaces were marked as areas with severe KRD in the study conducted by Bai et al. [15] (Table 1). Moreover, areas with an Exposed Bedrock Rate (EBR) of less than 30% were stated by Jiang et al. [4] as no desertification, while Bai et al. [15] categorized these areas into two groups as non-desertification or potential desertification areas (Table 1). In this study, the class intervals used by Jiang et al. [4] were preferred in the classification of KRD. Because of this complexity, a new classification approach was used in this study, in which the exposed rock rate and soil depth were evaluated together.

Table 1. Classification of exposed bedrock rate (EBR) in different KRD studies

Classification of Karst Rocky Desertification	EBR (Bai, et al. [15])	EBR (Jiang et al. [4])	EBR (Yang et al. [13])
No-Desertification	<%20	<30%	<10%
Potential	21%- 30%	-	-
Mild	31%- 50%	30%- 50%	10%- 30%
Moderate	51%- 70%	50%- 70%	30%- 50%
Severe	71%- 90%	> 70%	50%- 70%
Very Severe	> 91%	-	> 70%

In recent years, remote sensing (RS) methods have replaced labor-intensive and costly traditional methods in monitoring KRD [14,16]. RS methods provide low-cost data collection, wide area coverage and spatial continuity [8].

In the literature, normalized difference spectral indices are the most popular practices for ecological planning that are often used for the detection of Land Use/Land Cover Change and Land Surface Temperature studies which are based on similar conditions to occur KRD [17]. Monitoring, mapping and grading of KRD with RS methods are basically based on determining the land exposure rate (Exposed Bedrock Rate) and vegetation cover rate [18]. Visual interpretation and computer-aided image processing were emphasized in the first studies to detect KRD with the help of satellite images [14]. The advantage of spectral indices over other methods is that they give fast results in monitoring KRD in large areas without classification [14]. In some studies, the best performing indices that gave good results for monitoring KRD were retrieved by spectral unmixing to obtain more effective results on the image in mapping KRD [5]. One of the methods with high accuracy rates in determining the KRD is the support vector machine method [19]. Sub-pixel modeling and machine learning methods (such as Support Vector Machine, Random Forest) were also used to distinguish bare karst surfaces and covered areas in complex areas [7]. SVM, which is used in the classification of karst rock desertification, has been used successfully in different classification

applications and in solving pattern recognition problems [20, 21].

Various indices, mixture analysis and machine learning methods have been used for monitoring KRD at the regional or local level [16]. The aim of this study is to determine the spectral indices and classification method that gives the best results in KRD monitoring and to prove the areas where karst rock desertification is intense in the study area. Moreover, this study compares whether classified spectral indices or different classification practices are more effective in mapping KRD. For this purpose, firstly statistical linear relationships between spectral indices revealing karst rocky desertification and field measurements (In-Situ investigation) of karst rocky desertification were tested in the study area. Afterward, the accuracy rates of the spectral indices which were classified according to the index values and directly applied classification approaches such as machine learning methods were calculated. In addition, examining the human activities that accelerate this problem in the study area is another subject to be clarified. The research questions to be answered in line with these purposes: Is there a statistically significant relation between the spectral indices and the rate of exposed bedrock? What are the most effective methods for the classification of Karst Rocky Desertification in the Mediterranean region of Türkiye? How did the relations between karst landscapes and human activities develop in the study area within the scope of desertification?

2. Method

2.1. Study area

Aksu Stream Basin is a good example of an area where the Mediterranean climate is effective and karstification is common. A large part of the research area is located on the Taurus Mountains mass, which is one of the biggest karst landscapes of Türkiye [22]. The Aksu Stream Basin is located between 36-38° north latitudes and 30-31° east longitudes based on its mathematical location (Figure 1).

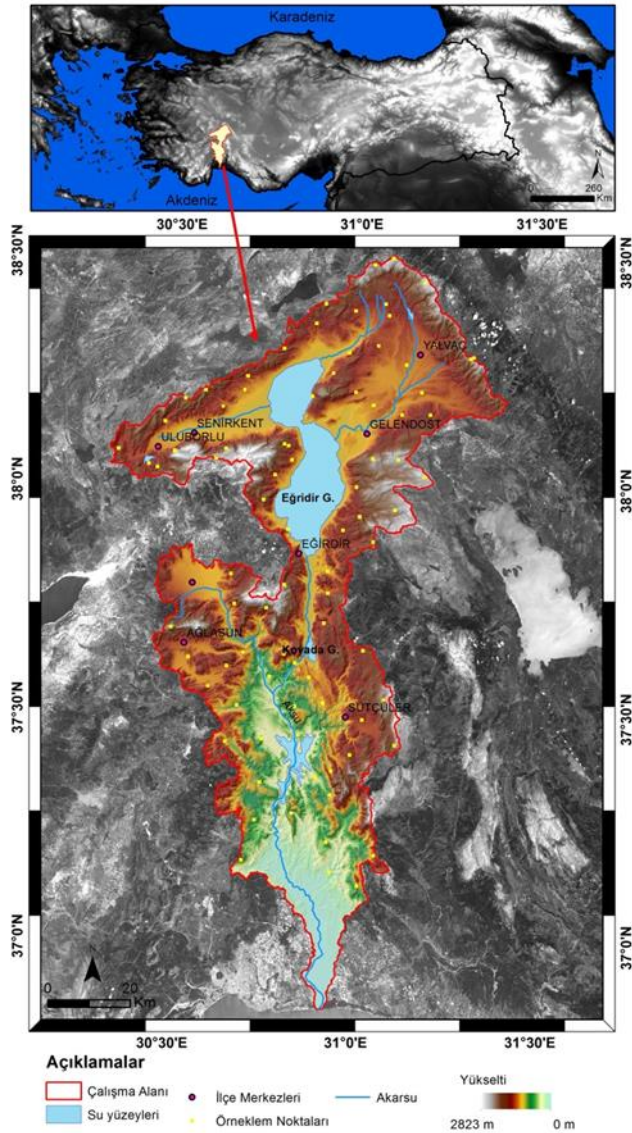


Figure 1. The location of research area and distribution of sample points

Gölcük Lake Basin was not included in the research boundaries as a result of which the boundaries of the research area were determined as 6850 km². Aksu Stream Basin is the largest sub-basin of Antalya Basin, which is one of the 25 major basins of Türkiye [23]. The formations of the land in the Aksu Stream Basin and its immediate surroundings present quite different spreading areas and lithological features. Limestone, which is very important in the formation of the KRD, dominates the study area. Limestone generally consists of units stratified in different formations of Triassic, Jurassic and Cretaceous ages [24]. Karst structures have been shown in the calcareous units indicating a suitable environment for the progress of the KRD in the study area.

Another factor affecting vegetation distribution in terms of KRD is climate. It is not feasible to reach a conclusion that a typical Mediterranean Climate is effective in the entire Aksu Stream Basin. Considering the monthly temperature values, it is known that the annual average temperature in the Western Mediterranean Region is 12.1-12.6 °C in the high regions, the sea impact is effective, and it is in the range of 12.7-13.9 °C in low altitude areas [25]. In the Aksu Stream Basin, the winter season is generally very rainy and humid, the summers are hot and dry, the spring is unstable in terms of precipitation, and the autumn season gains a character similar to the winter season [26].

2.2. Data

Landsat 8 OLI images presented by the United States Geological Survey (<http://usgs.com>) were used in this study, in which RS methods were employed for monitoring KRD. Landsat 8 satellite was launched by the National Aeronautics and Space Administration on February 11, 2013 with the addition of OLI and a Thermal Infrared sensor [17]. Later, it was transferred to USGS for routine imaging operations [27]. In the selection of images representing the study area, attention was paid to witness that the vegetation period has ended and the study area boundaries are completely cloudless (Table 2). In the next stages, pre-editing operations were performed on the images. The FLAASH (Fast Line-of-Sight Atmospheric Analysis of Hypercubes) tool was used for atmospheric and radiometric arrangements. Lakes in vector data format and non-karst areas obtained from 1/25000 scale geology maps created by MTA (Mining Technical Exploration) were excluded from the combined maps.

Table 2. Landsat 8 OLI images used in the study

Date	Image ID	Column	Row	Sun Angle	Cloud Rate (%)
1 July 2019	LC81780332019182LGN00	178	33	66.02	0.09
1 July 2019	LC81780342019182LGN00	178	34	66.59	1

One of the most important factors in determining the areas where KRD is effective is the exposed bedrock rate. In the determination of EBR, a relationship is established as the EBR increases as the vegetation cover rate decreases. The vegetation cover rate was determined by forest stands obtained from the General Directorate of

Forestry with the help of fieldwork from sampling points (Figure 1). Parameters which contained in forest stands such as average stand height and their distribution are repeated applications [28]. Horizontal vegetation cover in forest stands was determined as separating vegetation into 10x30 or 20x20 diameters with a peak frequency

meter [29]. Soil depth, which is another parameter used in the classification of KRD, was determined with the help of 82 field measurements with a soil auger (Figure 2). In the classification of images, 50 sample points were used for the training process and 32 measurements were utilized for ground truth accuracy.



Figure 2. A view from sampling with a 100cm auger to determine soil depth.

2.3. Method

The methods used in this study for monitoring KRD are Spectral Indices, Dimidiate Pixel Model, Multiple Spectral Mixture Analysis and Support Vector Machine. To understand how effective the spectral indices and sub-pixel segmentation are in monitoring KRD, the linear relationships between field measurements (rock ratio calculated using the tree cover ratio and soil depth) and the indices were tested with simple linear-regression analysis within the scope 82 sampling points (Eşitlik 1).

$$Y = a + b \cdot x \quad (1)$$

The indices that are frequently used in KRD monitoring studies are:

2.3.1. Karst bare-rock index (KBRI)

The methods applied in KRD are mainly based on the principle of distinguishing vegetation, bedrock surface and soil surface from each other [18]. In this method, the spectral difference between bare rock and other types of land cover becomes evident in the SWIR1 (Landsat 8-OLI image band 6) band (Eşitlik 2). As the index results obtained by making use of this relationship between the bands approach +1 the severity of KRD increases.

$$KBRI = \frac{pSWIR1 - pNIR}{20 \times \sqrt{pSWIR1 + pNIR}} \quad (2)$$

2.3.2. Normalized difference rock index (NDRI)

This index, derived by Huang and Cai [30] is calculated based on the difference between the strong reflection of visible radiation (band 3) and the complete

absorption of mid-infrared wavelengths (band 5) by water. In this method, it is accepted that KRD increases when the results are negative values, and decreases when the results are positive (Eşitlik 3).

$$NDRI = \frac{pNIR - pGreen}{pNIR + pGreen} \quad (3)$$

2.3.3. Carbonate rock index 2 (CRI2)

This index was prepared by Xie et al. [31] based on the logic that blue and near infrared bands are more effective in reflecting the vegetation cover with soil. In the results obtained by means of this index, karst landscapes become more pronounced in areas where reflection values decrease (Eşitlik 4).

$$CRI2 = \frac{pBlue - pNIR}{pBlue + pNIR} \quad (4)$$

2.3.4. Normalized difference built-up index (NDBI)

NDBI is one of the indices referenced in the literature for determining KRD [14]. This indice was applied with the use of SWIR1 and NIR bands (Eşitlik 5). The results mean that as the areas where positive values are calculated with NDBI approach up to + 1, the severity of KRD increases.

$$NDBI = \frac{pSWIR1 - pNIR}{pSWIR1 + pNIR} \quad (5)$$

2.3.5. Normalized difference vegetation index (NDVI)

NDVI is an index used to determine vegetation cover based on the relationship between the near infrared and red bands (Eşitlik 6). these values are close to +1 means that there is dense vegetation in the field, while being close to -1 means that the leaves lose their vitality or the vegetation is sparse [32]. In a region where NDVI shows negative values mean desertification has increased whereas the positive values are not observed below 0.2 [33].

$$NDVI = \frac{pNIR - pRed}{pNIR + pRed} \quad (6)$$

Another method preferred in KRD monitoring is Dimidiate Pixel Model. This model is generally used for the calculation of Fractional Vegetation Cover [7]. This method is defined as the rate of vertical coverage of the vegetation cover with its projection on the ground surface. Other methods are MESMA and SVM Methods which show the highest accuracy in the literature.

2.3.6. Dimidiate pixel model (DPM)

This model is generally used to calculate fractional vegetation [19]. This method is defined as the rate of the vertical coverage of vegetation to its projection on the ground surface. The Dimidiate Pixel Model used to determine Fractional Vegetation is based on the

relationship between green vegetation and open soil surfaces (Eşitlik 7). Firstly, using NDVI, the areas devoid of vegetation were determined and $NDVI_{Soil}$ was calculated. The regions where vegetation reaches the highest values are calculated as $NDVI_{Vegetation}$:

$$DPM = (NDVI_{Vegetation} - NDVI_{Soil}) / (NDVI_{Vegetation} + NDVI_{Soil}) \quad (7)$$

2.3.7. Multiple endmember spectral mixture analysis (MESMA)

Spectral Mixture Analysis is used to create models of pixel reflections with linear or nonlinear approaches [34]. MESMA is used in studies in the literature for different purposes such as determining the bedrock surface [35], classifying vegetation cover [36], and drawing the boundaries of urban areas [37] (Eşitlik 8). The reason why MESMA was preferred in addition to spectral indices in this study is its high performance in the determination of KRD in previous studies [7].

$$R_i = \sum_{k=1}^n f_k R_{ik} + \varepsilon_i \quad (8)$$

2.3.8. Support Vector Machine (SVM)

The Support Vector Machine approach is used to classify images using remote sensing methods and statistical methods [38]. This method tries to find the most suitable sub-pixels between classes by making use of training values [39]. The United States Geological Survey and European Space Agency use different machine learning algorithms including SVM for Spectral Feature extraction [40]. Also, thanks to this method, good classification accuracy with multi-spectral bands such as Landsat images is obtained [41].

KRD Criteria: The criteria for determining areas where KRD is effective in the research area were evaluated by dividing it into 4 classes. Vegetation cover, EBR and soil depth were evaluated together for the classification of KRD (Table 3). The first of these are areas without desertification where the vegetation cover is alive and soil depth is high. Other classes are regions where desertification is mild, moderate and severe. Samples belonging to these four classes in the research area can be easily distinguished in field studies (Figure 3).

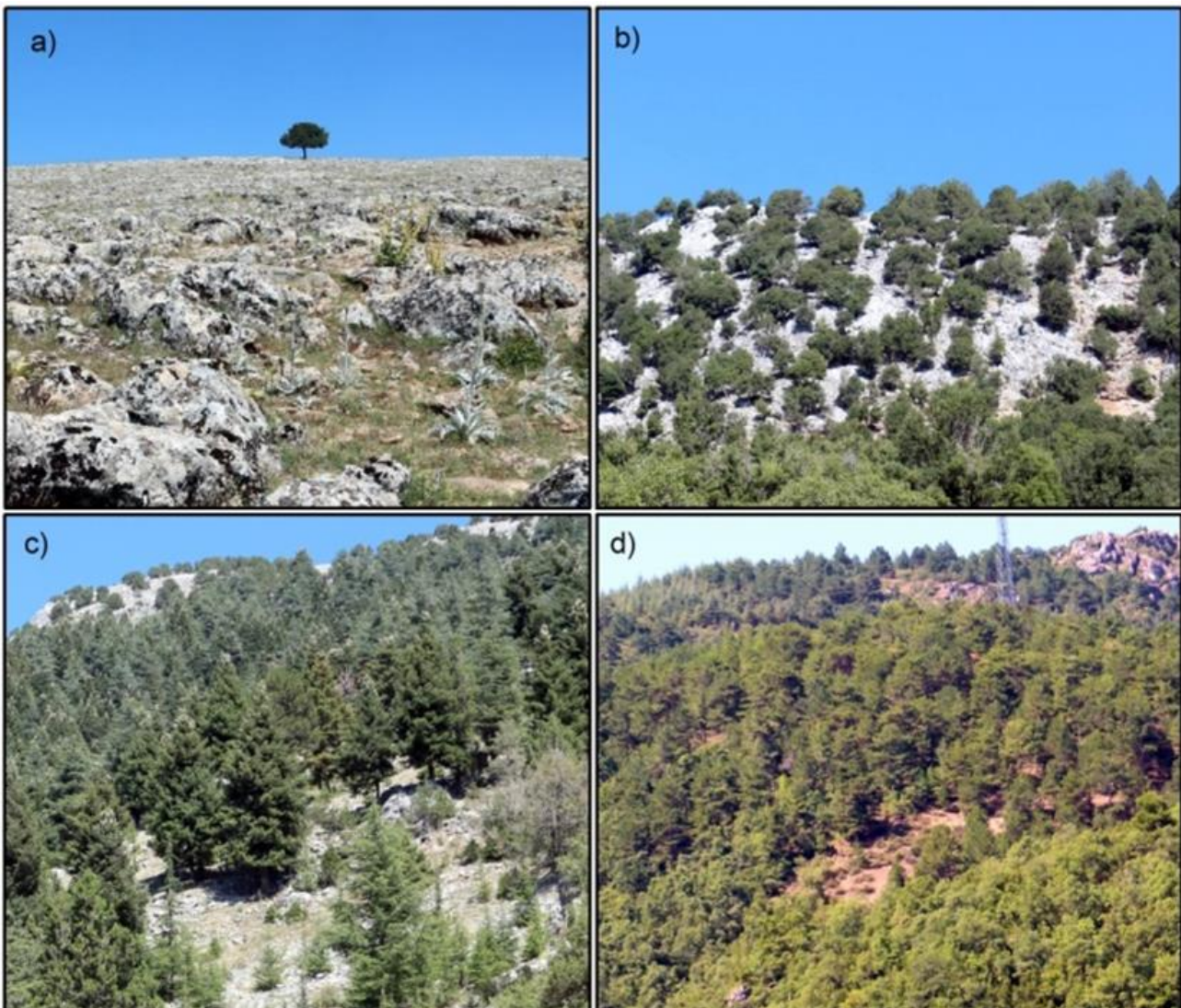


Figure 3. The views from different environments in study area of KRD in the research area; a) Severe KRD b) Moderate KRD c) mild KRD d) no KRD

Table 3. The criteria used in the classification of KRD in this study

Karst Rocky Desertification Classes	Exposed Bedrock Rate (%)	Vegetation Cover (%)	Soil Depth (cm)
No-Desertification	< %20	>80%	More than 75 cm
Mild	20% - 50%	%51-%80	20 -75 cm
Moderete	50%- 80%	20%- 50%	20-75 cm
Severe	> %80	< %20	Less than 20 cm

The performances of all indices used in this study were carried out by statistically testing their accuracy according to their percentage of bedrock. Thus, determination coefficients (R^2) were calculated between index results and spatial measurements (Eşitlik 9).

$$R^2 = \beta_0 + \beta_1.X + \epsilon \quad (9)$$

Within the scope of the classification of the results obtained from the methods applied for determining the KRD, determination of manual class ranges, Iso Clustered Unsupervised Classification, MESMA and Support Vector Machine methods were used. Accuracy evaluations of the classified data, 32 out of the 82 randomly selected sample points, were performed by calculating the Kappa Coefficient (Eşitlik 10).

$$K = \frac{P(o) - P(e)}{1 - P(e)} \quad (10)$$

3. Results

KRD develops in karst landscapes, where there is weak vegetation, vulnerable soil and warm-rainy climate conditions. Considering that agricultural activities have been going on for thousands of years in Anatolia, it is not possible to analyze the land independent from human activities. The weakening of the vegetation, the sensitization of the soil by human processing, and the interaction of human and natural processes increase the KRD effect. In the Aksu Stream Basin, natural processes and human activities were effective jointly in the land to reach its current appearance.

3.1. Comparison exposed bedrock rate between spectral indices

In this study determined by field measurements, higher results were obtained in the linear relationship levels of the spectral indices results calculated. The linear relationship between the various Spectral Indices and Dimidiate Pixel Model results and the EBR obtained from the sample points was tested with the regression model (Figure 4). All of the Indices used for monitoring and mapping KRD have values between +1 and -1 (Figure 4). According to the results, high-level and statistically significant linear relationships were determined between the results of 4 methods and the Exposed Bedrock Rate. Among them, DPM and KBRI were determined to be statistically compatible with terrestrial measurements. There is a statistically positive correlation between EBR values and KBRI, CRI2 and

NDBI results, while there is a negative correlation between NDRI, NDVI and DPM. Highly significant relationships were determined between EBR obtained from sample points and the results of KBRI, NDBI, NDVI and DPM methods (Figure 4). A lower level of linear relationship was found between the other indices NDVI and NDBI and spatial measurements. In this study, the indices in which a low-level linear relationship is determined with local measurements are NDRI and CRI2. The linear relationships at the level between the results obtained within the scope of determining the KRD in this study and the field measurements mean that most of these methods show moderate performance. It is seen that EBR could not represent the bedrock in estimation, but DPM results were successful in predicting EBR.

In all spectral index results of KRD, regions with severe desertification are expressed in red, and areas with healthy vegetation are expressed in green (Figure 5). Considering the results obtained in this study, although there is a difference between the values, some similarities appear in the general outlook (Figure 5). Considering that the best estimate for the estimation of EBR is DPM results, KRD increases from south to north and from west to east in the Aksu Stream Basin (Figure 5).

3.2. Classification of results

The situation that misleads the results obtained by RS methods for determining the KRD most and that causes the occurrence of error margin in classifications is the garrigue formations that develop on thin soil cover and spread continuously over the field. The fact that some areas determined in field observations where KRD is effective are covered with thin soil and garrigue cover which have a good value of vegetation reflection prevents the determination of desertification in these areas by satellite images (Figure 6).

Accuracy analyses of classifications performed within the scope of determining the areas where KRD is effective were carried out within the scope of control points. Accordingly, the reliability of agreement between local examinations carried out with the field studies and the classified results was tested (Table 4). The results presented within the scope of KRD in the research area were classified using the Spectral Indices of Iso-Cluster Unsupervised Classification, MESMA and SVM methods. The accuracy of the classes and spatial measurements were calculated with the Kappa Coefficient (Table 4).

According to these results, it was determined that the classification accuracy in MESMA and SVM methods was considerably higher.

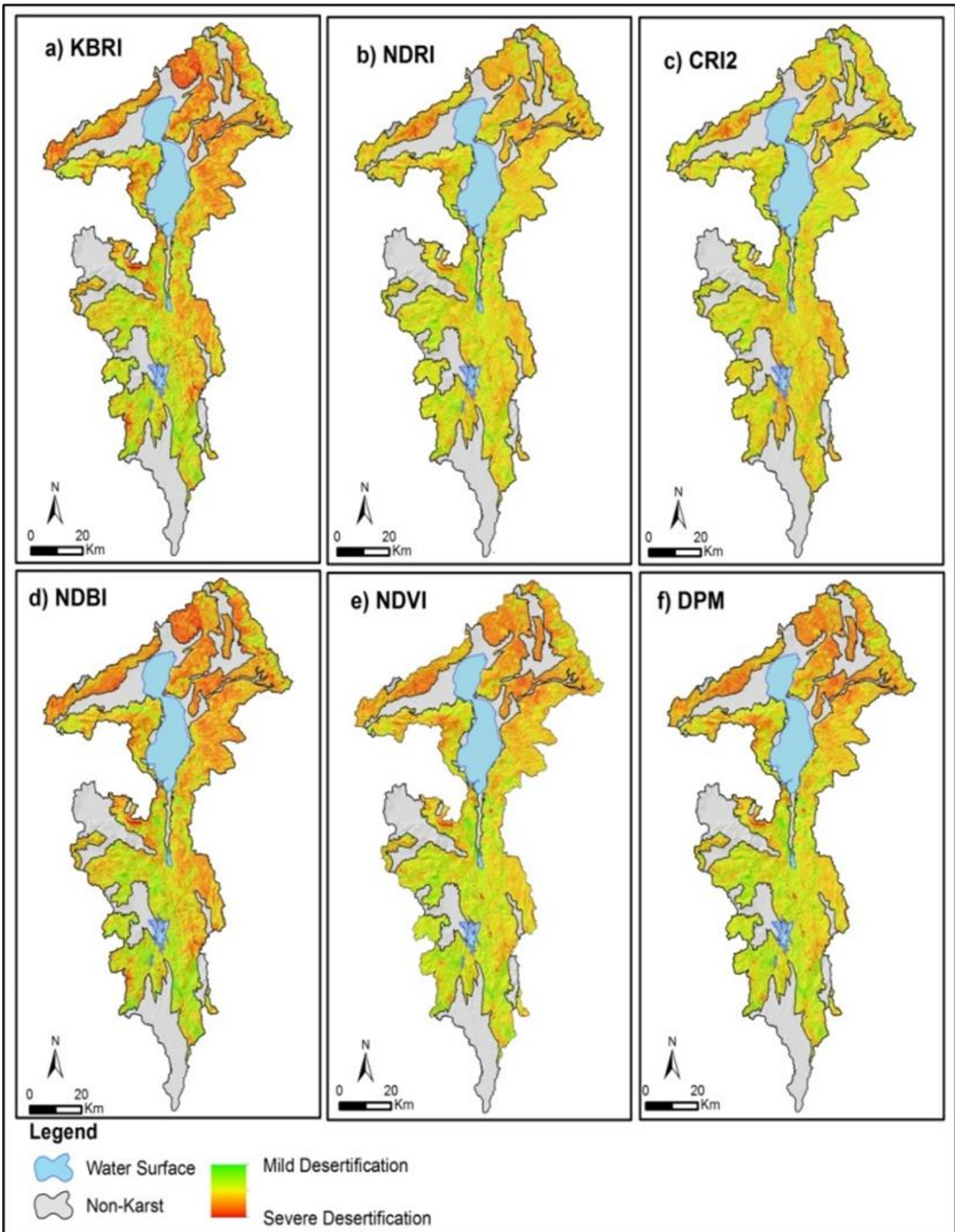


Figure 5. The results of methods used to assess KRD: a) Karst Bare Rock Index (KBRI), b) Normalized Difference Rock Index (NDRI), c) Carbonate Rock Index 2 (CRI2), d) Normalized Difference Build-Up Index (NDBI), e) Normalized Difference Vegetation Index (NDVI), f) Dimidiated Pixel Model (DPM)

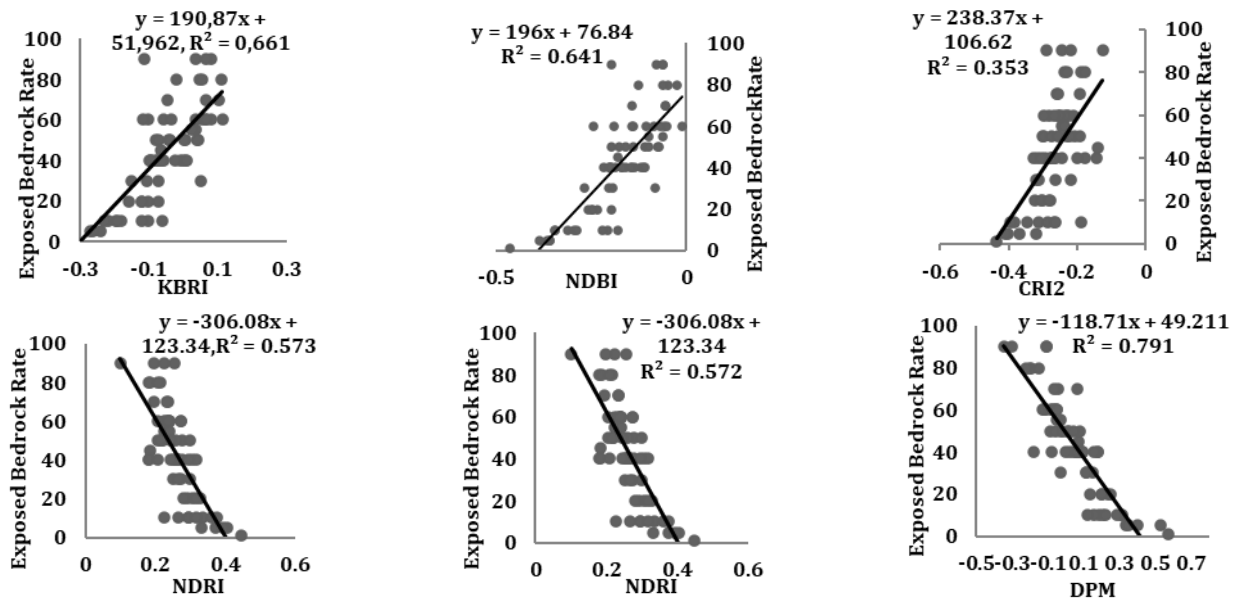


Figure 4. The Linear relationships between exposed bedrock rate and methods which used to assess KRD in this study

Table 4. Kappa coefficient of classification results

Classification	ISO-KBRI	ISO-NDRI	ISO-CR12	ISO-NDBI
Overall accuracy	0,65	0,61	0,55	0,61
Kappa	0,52	0,46	0,39	0,46
Classification	ISO-NDVI	ISO-DPM	MESMA	SVM
Overall accuracy	0,68	0,69	0,75	0,88
Kappa	0,56	0,57	0,65	0,81



Figure 6. A view of the uninterrupted garrigue formations that prevent to assess KRD based on RS methods around the Uluğbey settlement.

According to the classification results with the highest statistical accuracy, it is seen that the SVM is effective in a significant part of the research area. High-accuracy results show that KRD is high around Lake Eğirdir (Figure 7).

One of the important findings in this study is not only direct measurements of some indexes defined as high accuracy to explain KRD level, but also high overall accuracy was determined when they were classified. In this study, it was concluded that the most effective

methods of KRD classification were MESMA and SVM which are two separate methods in the various classification methods used in this study.

3.3. The effects of KRD: Space and People

In the examinations carried out on the surfaces where KRD is effective in the research area, it is understood that human-induced effects accelerate this process. These effects are primarily seen in that the lands lose their productivity as a result of agricultural misuse and intensive land opening applications where the slope is increased (Figure 7). Uncontrolled human activities (overgrazing, improper agricultural practices and improper land use) and extreme natural events (fires) in karst lands play a critical role in desertification. To express the KRD process in the study area gradually, people first clear the area of vegetation where they will carry out agricultural activities. As agricultural activities are carried out in these areas where plowing activities are carried out, the topsoil is eroded. Over time, these areas are left to their fate as the yield decreases. The evidence of the abandonment of agricultural lands is piles of stones between rocks and grass (Figure 8). In this case, since there are sparse plants left to hold the soil cover in the field, bare rocky surfaces are exposed by erosion.

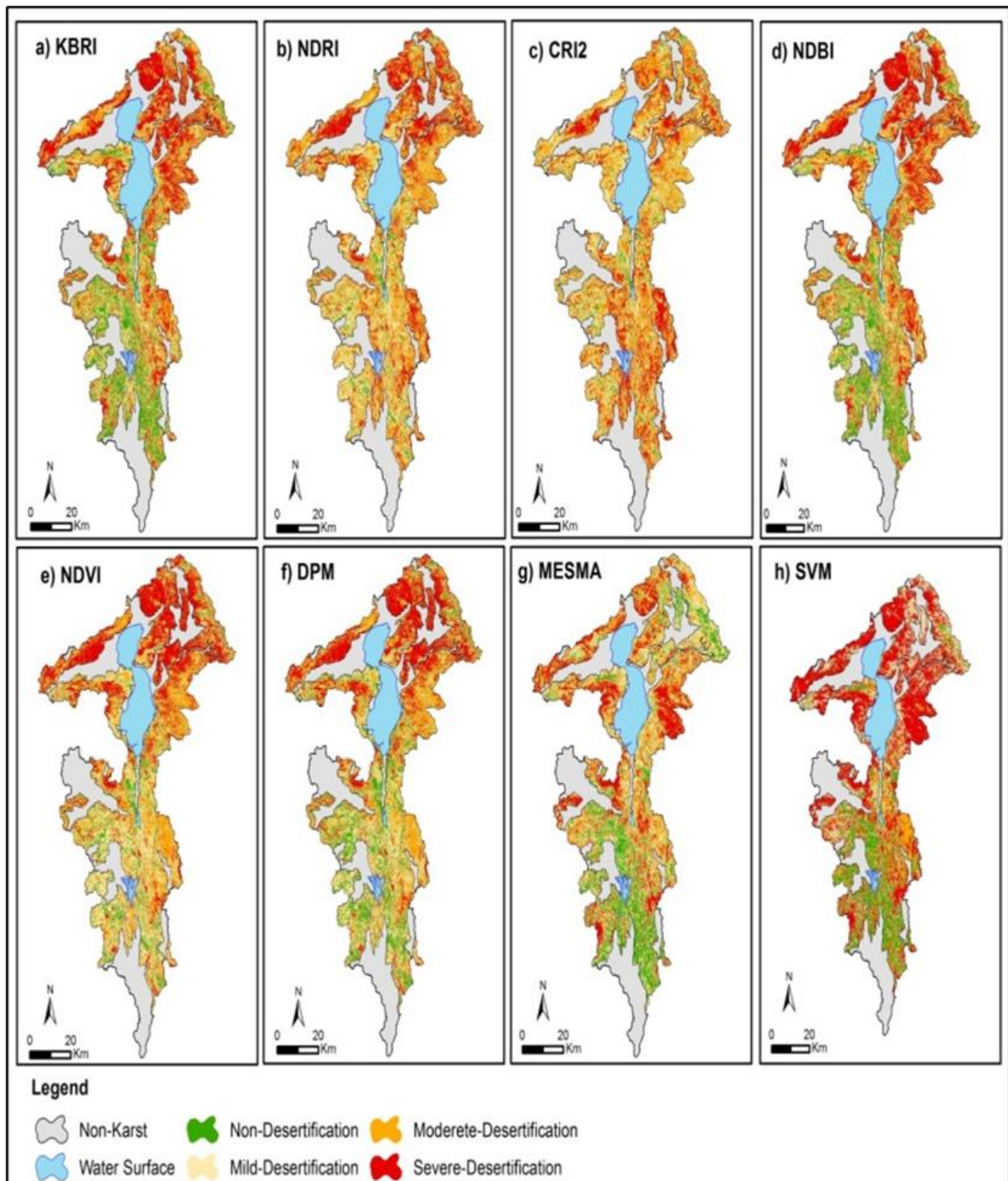


Figure 7. Classification ranges which of KRD results created

4. Discussion

Considering the studies in the literature, it is seen that different results are obtained by using the spectral indices used within the scope of KRD [14, 16]. In terms of general uses, KBRI, NDRI, CRI2 and NDBI indices other than NDVI are used to monitor karst rock desertification. The main indicator for monitoring KRD is the prevalence of EBR in the field. In the literature, there have been many studies on determining the relationship between vegetation and bedrock with remote sensing methods [8, 9, 14, 16, 17, 31, 42].

Natural processes that are effective in the occurrence of KRD in the field are also associated with the slowing of

soil development due to the low silicate ratio caused by the geological structure of carbonate rocks [43]. The karst system becomes ecologically fragile due to slow soil development and weak vegetation in direct proportion to this situation [13]. In studies on KRD, classifications are made within the scope of vegetation status and open rocky surfaces [44]. Considering these classifications in general, Li and Wu [16] emphasize that mainly 4 classes can be mentioned in the study and it is stated that an absolute classification method is needed. Thus, by classifying the available data, it is possible to make more effective evaluations of how much of the area has been exposed to desertification and where this desertification is effective.

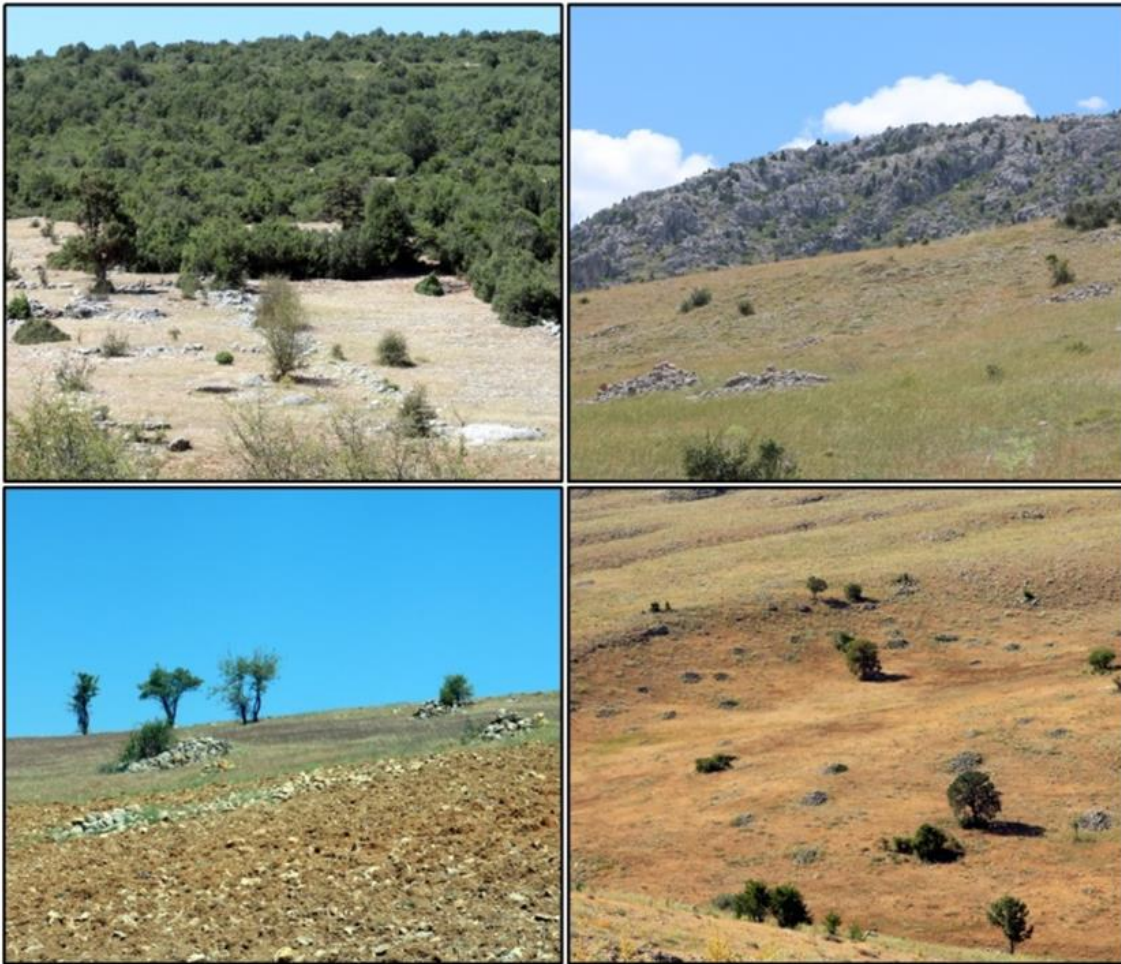


Figure 8. The views from areas where previously cultivated but not now used for agriculture due to desertification

Studies in the literature have reached similar results to the findings of this study, showing that rock exposure rate and vegetation contribute the most to karst rocky desertification inference [42].

Although desertification developed on rocks is not a situation that develops only on carbonate rocks, KRK also has very specific features [43]. This situation arises from the geological properties of karst surfaces. The high chemical dissolution (melting) levels of carbonate rocks slow down soil development [4].

As emphasized in the study by Li and Wu [16] within the scope of evaluating the effects of KRK, it is understood that a classification method is needed instead of spectral indices. In this study, a comparison was made between the spectral indices and the DPM model in terms of the determination of karst rocky desertification. This comparison revealed different results from the spectral indexes with a high accuracy rate, as in other studies in the DPM literature [7, 45].

Traditional methods (field studies) for monitoring karst rocky desertification mainly rely on field surveys, which require a quite deal of time and finance. Although using remote sensing images for monitoring karst rocky desertification is not limited by the topography, erosion or land cover, it also has disadvantages, including poor image quality (cloudiness), readily affected by human subjectivity, and strictly guaranteeing the accuracy [46]. In this study, field studies from traditional karst rocky desertification methods were also carried out in order to detect the inadequacies that may occur as well as the low

cost and fast decision-making processes of remote sensing. It has been determined that some areas determined in the field studies where KRK is effective are covered with thin soil and garig cover with good vegetation reflectance, and the determination of desertification in these areas by satellite images is prevented.

The most important reason for the natural integrity of the land is erosion becomes stronger as a result of human activities such as destroying vegetation, plowing and contracting roads [47].

Increasing erosion by removing vegetation due to reasons such as fires, overgrazing, improper agricultural practices and improper land use in the Mediterranean Basin is extremely effective KRK development [48, 49].

In addition, the Southern Anatolian mountains, which are described as Taurides, are generally composed of limestones. Widespread karstification in these areas has affected the people living here. Animal husbandry and agricultural activities carried out by people on these surfaces, which have a particularly difficult and faulty topography as karst, take place on the dolines, poljes, and paleo-valleys in these areas [50, 51]. In this study, it was determined that people gradually accelerate KRK directly in karst areas. First of all, people remove the vegetation on the surface where the soil is attached to the karst area. Then, they cultivate the areas with high soil thickness and process them as agricultural land. After the mobilized soil becomes susceptible to erosion, it is carried away by erosion processes and prepares the

ground for karst rock desertification. In the study, it was determined that people wanted to continue agriculture by collecting the rocks exposed in the agricultural lands and left the area as the yield decreased (Figure 8).

5. Conclusion

This study proposes mapping and monitoring of KRD development on karst landscapes in many parts of the World with different RS methods. In this study, high linear relationships were determined between some indices such as KBRI and EBR statistically; also, these indices gave high accuracy results when classified. This means that successful results could not be obtained with monitoring and classification of KRD with spectral indices. One of the possible reasons for not determining a statistically high linear relationship between spectral indices and KRD may be caused by bushes covering the surface. In addition to the poor results in monitoring and classification of KRD, it was determined that SVM (overall accuracy 88%) SVM and MESMA (overall accuracy 77%) methods were found to be successful at a good level. The possible reason why MESMA and SVM methods were more successful than spectral indices is the use of training series based on field measurements. It is understood that the classifications made by these two methods will be efficient in making long-term change detection analyses. In this way, classification results with the highest accuracy in the study area, the proportion of areas subject to severe karst desertification is 40%, those in moderate desertification process 17%, mild desertification 14% and non-desertification 29%.

According to the results, it has been revealed that KRD is quite effective in some parts of the study area. The results obtained in this study, draw attention to the decrease in KRD in the areas where sea impact increases, and in the higher parts, the KRD increases as we move towards the inland areas, similar to the Aksu Stream Basin. In the north of the study area, it was observed that the KRD is particularly effective in the high topography bordered by plain surface. It is noteworthy that the main reason why KRD is effective here is erosion. In addition, it is clearly observed in the field that agricultural production is not efficient enough in the areas where the KRD is effective. The areas with a high Exposed Bedrock Rate where people are trying to conduct agricultural activities make the agricultural conditions worse and reduce agricultural productivity. Uncontrolled agriculture in these lands causes bedrock outcrops to rise to the surface faster. The emergence of bedrock means changing the agricultural land and living conditions for rural people. Thus, increasing difficulties such as inefficiency and limited product diversity show their conditions in rural settlements with many vacant households in the study area. Also, this situation can be accepted as a sign that KRD is effective in the high and sloping parts of the Karst regions in Türkiye.

Acknowledgement

The authors want to thank U.S. Geological Survey for presenting the free access to the Landsat-8 images.

Author contributions

Çağan Alevkayali: Writing-Original draft preparation, Methodology, Software, Data curation, Fieldwork, Validation, Investigation and Visualization; **Onur Yayla:** Fieldwork, Investigation, Visualization and Writing **Yıldırım Atayeter:** Investigation, Fieldwork, Writing and Editing.

Conflicts of interest

The authors declare no conflicts of interest.

References

1. Parise, M., Gabrovsek, F., Kaufmann, G., & Ravbar, N. (2018). Recent advances in karst research: from theory to fieldwork and applications. *Geological Society, London, Special Publications*, 466(1), 1-24.
2. Erinc, S. (2002). Jeomorfoloji II. İstanbul: DER Yayınları.
3. Theilen-Willige, B., Ait Malek, H., Charif, A., El Bchari, F., & Chaïbi, M. (2014). Remote sensing and GIS contribution to the investigation of karst landscapes in NW-Morocco. *Geosciences*, 4(2), 50-72.
4. Jiang, Z., Lian, Y., & Qin, X. (2014). Rocky desertification in Southwest China: Impacts, causes, and restoration. *Earth-Science Reviews*, 132, 1-12.
5. Zhang, X., Shang, K., Cen, Y., Shuai, T., & Sun, Y. (2014). Estimating ecological indicators of karst rocky desertification by linear spectral unmixing method. *International Journal of Applied Earth Observation and Geoinformation*, 31, 86-94.
6. Ekmekçi, M. (2005). Karst in Turkish Thrace: compatibility between geological history and karst type. *Turkish Journal of Earth Sciences*, 14(1), 73-90.
7. Qi, X., Zhang, C., & Wang, K. (2019). Comparing remote sensing methods for monitoring karst rocky desertification at sub-pixel scales in a highly heterogeneous karst region. *Scientific reports*, 9(1), 1-12.
8. Yue, Y. M., Wang, K. L., Liu, B., Li, R., Zhang, B., Chen, H. S., & Zhang, M. Y. (2013). Development of new remote sensing methods for mapping green vegetation and exposed bedrock fractions within heterogeneous landscapes. *International journal of remote sensing*, 34(14), 5136-5153.
9. Yue, Y. M., Wang, K. L., Zhang, B., Jiao, Q. J., Liu, B., & Zhang, M. Y. (2012). Remote sensing of fractional cover of vegetation and exposed bedrock for karst rocky desertification assessment. *Procedia Environmental Sciences*, 13, 847-853.
10. Zhang, C., Qi, X., Wang, K., Zhang, M., & Yue, Y. (2017). The application of geospatial techniques in monitoring karst vegetation recovery in southwest China: A review. *Progress in Physical Geography*, 41(4), 450-477.
11. Xiong, Y. J., Qiu, G. Y., Mo, D. K., Lin, H., Sun, H., Wang, Q. X., ... & Yin, J. (2009). Rocky desertification and its causes in karst areas: a case study in Yongshun County, Hunan Province, China. *Environmental Geology*, 57, 1481-1488.

12. Liu, Y., Wang, J., & Deng, X. (2008). Rocky land desertification and its driving forces in the karst areas of rural Guangxi, Southwest China. *Journal of Mountain Science*, 5, 350-357.
13. Yang, W., Chu, W., & Zhou, L. (2019). Evaluating the impact of karst rocky desertification on regional climate in Southwest China with WRF. *Theoretical and Applied Climatology*, 137, 481-492.
14. Pei, J., Wang, L., Huang, N., Geng, J., Cao, J., & Niu, Z. (2018). Analysis of Landsat-8 OLI imagery for estimating exposed bedrock fractions in typical karst regions of Southwest China using a karst bare-rock index. *Remote Sensing*, 10(9), 1321.
15. Bai, X. Y., Wang, S. J., & Xiong, K. N. (2013). Assessing spatial-temporal evolution processes of karst rocky desertification land: indications for restoration strategies. *Land Degradation & Development*, 24(1), 47-56.
16. Li, S., & Wu, H. (2015). Mapping karst rocky desertification using Landsat 8 images. *Remote sensing letters*, 6(9), 657-666.
17. Guha, S., & Govil, H. (2020). Estimating the seasonal relationship between land surface temperature and normalized difference bareness index using Landsat data series. *International Journal of Engineering and Geosciences*, 7(1), 9-16.
18. Wang, H., Li, Q., Du, X., & Zhao, L. (2018). Quantitative extraction of the bedrock exposure rate based on unmanned aerial vehicle data and Landsat-8 OLI image in a karst environment. *Frontiers of Earth Science*, 12, 481-490.
19. Xu, E. Q., Zhang, H. Q., & Li, M. X. (2015). Object-based mapping of karst rocky desertification using a support vector machine. *Land Degradation & Development*, 26(2), 158-167.
20. Kaynarca, M., Demir, N., & San, B. T. (2020). Yeraltı Suyu Kaynaklarının Uzaktan Algılama ve CBS Teknikleri Kullanarak Modellenmesine Yönelik bir Yaklaşım: Kırkgöz Havzası (Antalya). *Geomatik*, 5(3), 241-245.
21. Reis, H. Ç., & Yılanlı, G. (2020). Destek vektör makineleri ve NDVI kullanarak pamuk ekili alanların tespiti: Harran ovası örneği. *Türkiye Uzaktan Algılama Dergisi*, 2(1), 29-41.
22. Şimşek, M., Utlı, M., Poyraz, M., & Öztürk, M. Z. (2019). Geyik Dağı kütlesinin yüzey karstı jeomorfolojisi ve kütle üzerindeki karst-buzul jeomorfolojisi ilişkisi. *Ege Coğrafya Dergisi*, 28(2), 97-110.
23. Tokgözlü, A., & Özkan, E. (2018). Taşkın risk haritalarında AHP yönteminin uygulanması: Aksu Çayı Havzası örneği. *Süleyman Demirel Üniversitesi Fen-Edebiyat Fakültesi Sosyal Bilimler Dergisi*, (44), 151-176.
24. Atayeter, Y. (2005). *Aksu Çayı havzası'nın jeomorfolojisi*. Fakülte Kitabevi.
25. Karatepe, Y., Özçelik, R., Gürlevik, N. E. V. Z. A. T., Yavuz, H., & Kiriş, R. (2014). Batı Akdeniz'de farklı yetiştirme ortamı bölgelerindeki kızılçam (*Pinus brutia* Ten.) ormanlarının vejetasyon yapısının ekolojik değerlendirilmesi. *Süleyman Demirel Üniversitesi Orman Fakültesi Dergisi*, 15(1), 1-8.
26. Atayeter, Y. (2011). Eğirdir Gölü Depresyonu ve Yakın Çevresinin Fiziki Coğrafya Özellikleri. Isparta. Fakülte Yayınları
27. Roy, D. P., Wulder, M. A., Loveland, T. R., Woodcock, C. E., Allen, R. G., Anderson, M. C., ... & Zhu, Z. (2014). Landsat-8: Science and product vision for terrestrial global change research. *Remote sensing of Environment*, 145, 154-172.
28. Sefercik, U. G., Ateşoğlu, A., & Atalay, C. (2021). Orman meşcere yükseklik haritası üretiminde hava kaynaklı lazer tarama performans analizi. *Geomatik*, 6(3), 179-188.
29. Genç, M., Kasarcı, E., & Kaya, C. (2012). Meşcere Kuruluşu Araştırmaları Üzerine Silvikültürel Bir Değerlendirme. *Artvin Çoruh Üniversitesi Orman Fakültesi Dergisi*, 13(2), 291-303.
30. Huang, Q., & Cai, Y. (2009). Mapping karst rock in Southwest China. *Mountain Research and Development*, 29(1), 14-20.
31. Xie, X., Du, P., Xia, J., & Luo, J. (2015). Spectral indices for estimating exposed carbonate rock fraction in karst areas of southwest China. *IEEE Geoscience and Remote Sensing Letters*, 12(9), 1988-1992.
32. Sabuncu, A., & Ozener, H. (2019). Detection of burned areas by remote sensing techniques: İzmir Seferihisar Forest fire case study. *Journal of Natural Hazards and Environment*, 5(2), 317-326.
33. Xu, D., Kang, X., Qiu, D., Zhuang, D., & Pan, J. (2009). Quantitative assessment of desertification using Landsat data on a regional scale—a case study in the Ordos Plateau, China. *Sensors*, 9(3), 1738-1753.
34. Somers, B., Asner, G. P., Tits, L., & Coppin, P. (2011). Endmember variability in spectral mixture analysis: A review. *Remote Sensing of Environment*, 115(7), 1603-1616.
35. Bedini, E., Van Der Meer, F., & Van Ruitenbeek, F. (2009). Use of HyMap imaging spectrometer data to map mineralogy in the Rodalquilar caldera, southeast Spain. *International Journal of Remote Sensing*, 30(2), 327-348.
36. Lippitt, C. L., Stow, D. A., Roberts, D. A., & Coulter, L. L. (2018). Multidate MESMA for monitoring vegetation growth forms in southern California shrublands. *International journal of remote sensing*, 39(3), 655-683.
37. Powell, R. L., & Roberts, D. A. (2008). Characterizing variability of the urban physical environment for a suite of cities in Rondonia, Brazil. *Earth Interactions*, 12(13), 1-32.
38. Moughal, T. A. (2013, June). Hyperspectral image classification using support vector machine. In *journal of physics: conference series* (Vol. 439, No. 1, p. 012042). IOP Publishing.
39. Tzotsos, A., & Argialas, D. (2008). Support vector machine classification for object-based image analysis. *Object-based image analysis: Spatial concepts for knowledge-driven remote sensing applications*, 663-677.
40. Benbahria, Z., Sebari, I., Hajji, H., & Smiej, M. F. (2021). Intelligent mapping of irrigated areas from Landsat 8 images using transfer learning. *International Journal of Engineering and Geosciences*, 6(1), 40-50.

41. Melgani, F., & Bruzzone, L. (2004). Classification of hyperspectral remote sensing images with support vector machines. *IEEE Transactions on geoscience and remote sensing*, 42(8), 1778-1790.
42. Pu, J., Zhao, X., Dong, P., Wang, Q., & Yue, Q. (2021). Extracting information on rocky desertification from satellite images: A comparative study. *Remote Sensing*, 13(13), 2497.
43. Wang, S. J., Liu, Q. M., & Zhang, D. F. (2004). Karst rocky desertification in southwestern China: geomorphology, landuse, impact and rehabilitation. *Land degradation & development*, 15(2), 115-121.
44. Xu, E., Zhang, H., & Li, M. (2013). Mining spatial information to investigate the evolution of karst rocky desertification and its human driving forces in Changshun, China. *Science of the Total Environment*, 458, 419-426.
45. Dai, G., Sun, H., Wang, B., Huang, C., Wang, W., Yao, Y., ... & Zhang, Z. (2021). Assessment of karst rocky desertification from the local to regional scale based on unmanned aerial vehicle images: A case-study of Shilin County, Yunnan Province, China. *Land Degradation & Development*, 32(18), 5253-5266.
46. Zhang, Y., Tian, Y., Li, Y., Wang, D., Tao, J., Yang, Y., ... & Wu, L. (2022). Machine learning algorithm for estimating karst rocky desertification in a peak-cluster depression basin in southwest Guangxi, China. *Scientific Reports*, 12(1), 19121.
47. Dindaroğlu, T., & Çelik, H. (2019). Yeşil kuşak orman ekosistemlerindeki orman parçalılığının bazı toprak özellikleri üzerindeki etkilerinin araştırılması (Kahramanmaraş Ahir dağı örneği). *Kahramanmaraş Sütçü İmam Üniversitesi Tarım ve Doğa Dergisi*, 22(2), 322-332.
48. Chong, G., Hai, Y., Zheng, H., Xu, W., & Ouyang, Z. (2021). Characteristics of changes in karst rocky desertification in southern and western china and driving mechanisms. *Chinese Geographical Science*, 31, 1082-1096.
49. Haktanir, K., Karaca, A., & Omar, S. M. (2004). The prospects of the impact of desertification on Turkey, Lebanon, Syria and Iraq. In *Environmental Challenges in the Mediterranean 2000–2050: Proceedings of the NATO Advanced Research Workshop on Environmental Challenges in the Mediterranean 2000–2050 Madrid, Spain 2–5 October 2002* (pp. 139-154). Springer Netherlands.
50. Ballut, C., & Faivre, S. (2012). New data on the dolines of Velebit Mountain: An evaluation of their sedimentary archive potential in the reconstruction of landscape evolution. *Acta Carsologica*, 41(1).
51. Şimşek, M., Öztürk, M. Z., Doğan, U., & Mustafa, U. T. L. U. (2021). Toros polyelerinin morfometrik özellikleri. *Coğrafya Dergisi*, (42), 101-119.



© Author(s) 2023. This work is distributed under <https://creativecommons.org/licenses/by-sa/4.0/>